Published in "Physical Review B 74: 104513, 2006"
which should be cited to refer to this work.

Isotope effect on the optical phonons of $YBa_2Cu_4O_8$ studied by far-infrared ellipsometry and Raman scattering

A. Trajnerowicz,[1,2] A. Golnik,[1,2] C. Bernhard,[2,3] L. Machtoub,[2] C. Ulrich,[2] J. L. Tallon,[4] and M. Cardona[2]
[1]*Institute of Experimental Physics, Warsaw University, Hoża 69, 00-681 Warsaw, Poland*
[2]*Max-Planck Institut für Festkörperforschung, Heisenbergstr. 1, D-70569 Stuttgart, Germany*
[3]*Department of Physics, University of Fribourg, Chemin du Musée 3, CH-1700 Fribourg, Switzerland*
[4]*New Zealand Institute for Industrial Research, P.O. Box 31310, Lower Hutt, New Zealand*

The phonon spectra of $YBa_2Cu_4O_8$ polycrystalline samples with different isotope substitution for Ba, Cu, and O have been studied using far-infrared ellipsometry and Raman scattering. The observed isotope shifts of Raman- and infrared-active phonons provide insight into their relative Ba, Cu, and O normal mode content. This allows us to examine mode eigenvectors obtained from lattice dynamical calculations using *ab initio* electronic structures based on the full potential linear muffin-tin-orbital within the local density approximation. Our Raman results demonstrate that the 104 cm^{-1} A_g phonon is only very weakly mixed, representing almost pure Ba vibrations. Correspondingly the 151 cm^{-1} phonon represents pure Cu vibrations. The 339, 436, and 498 cm^{-1} phonon modes involve mainly O vibrations. Considerable Cu-O mixing takes place in the case of the A_g phonons at 257 and 605 cm^{-1} and for the B_{3g} phonon at 314 cm^{-1}. These results are in good agreement with the *ab initio* calculations. The far-infrared experiments reveal that the modes with energies of 115, 297, 502, and 592 cm^{-1} are mixed vibrations of O and Cu atoms. The phonon mode at 130 cm^{-1} corresponds to a Ba-Cu-O complex whereas the modes at 191 and 357 cm^{-1} reflect almost pure Cu and O vibrations, respectively.

PACS number(s): 74.25.Kc, 74.72.Bk, 74.25.Gz

I. INTRODUCTION

High-T_c superconductivity (HTSC) in the cuprates is one of the most curious phenomena in today's solid-state Physics. The underlying mechanism is still not understood and many new experiments are being conducted in order to reveal its origin. Among other important issues the role of the electron-phonon coupling remains a controversial topic. Concerning the superconducting pairing mechanism it has recently been debated whether strong electronic correlation effects could give rise to a significant enhancement of the electron-phonon coupling.[1,2] Alternatively, based on the observation of a growing isotope effect on T_c towards the underdoped side of the phase diagram, it has also been argued that the electron-phonon interaction may be involved in stabilizing competing orders such as charge density wave or charge ordered states.[3–5]

A prerequisite for a successful phonon-based microscopic theory is the assignment of the various phonon modes of these rather complex materials, including the knowledge about the vibration eigenvectors for the participating ions. Another motivation for a reliable assignment of the phonon modes comes from the observation of large local electric field effects in the *c*-axis response of various HTSC materials, especially in the superconducting state.[6,7] It has been established that the strongly anisotropic and anomalous electronic response of the HTSC can give rise to substantial modifications of the local electric fields even within a single primitive cell, i.e., on a nanometer scale. The electronic and the ionic degrees of freedom are entangled here in a very unusual manner which strongly depends on the ionic displacement pattern of the various phonon modes. Relevant information can be obtained by comparing the predictions from theoretical calculations based on the shell model or *ab initio* methods with the experimentally observed shifts of the phonon modes upon isotopic replacement of the various constituent ions.

There have been several reports about isotopic phonon shifts in high-T_c superconductors. The majority of these reports deal with the replacement of ^{16}O by ^{18}O, which can even be substituted in a site-selective way.[8–12] For the heavier elements Y, Ba, and Cu the available information is scarce. Mascarenhas *et al.*[13] and Irwin *et al.*[14] have compared Raman spectra of YBa_2, $^{nat}Cu_3O_7$, and $YBa_2{}^{65}Cu_3O_7$ ceramics. Strach *et al.*[15] investigated the coupling of Ba (121 cm^{-1}) and Cu vibrations for two A_g modes also using the Raman technique. Henn *et al.*[16] compared Raman data with infrared measurements obtained by far-infrared ellipsometry for $YBa_2Cu_3O_7$ with different isotopic compositions of Ba and Cu.

The structure of $YBa_2Cu_4O_8$ ($Y124$), a slightly underdoped HTSC material with T_c=80 K, is closely related to the one of the better known $YBa_2Cu_3O_{7-\delta}$ ($Y123$). The main difference between $Y124$ and $Y123$ is related to the double CuO chains in $Y124$ as compared to the single CuO chain layer in $Y123$. This increases the number of atoms in the $Y124$ primitive cell to 15 (see Fig. 1). The $Y124$ structure belongs to the D_{2h} symmetry point group. The primitive cell of $Y124$ contains two consecutively stacked $Y123$ blocks that are shifted by half a lattice parameter along the *b* axis direction (see Fig. 1). Unlike in $Y123$, the Cu and O atoms in the CuO double chains of Y124 are not at inversion symmetry centers and thus give rise to additional Raman active vibrations. This enhances the number of even symmetry (Raman-active) zone center phonon modes (k=0) from 15 in $Y123$ to 21 in $Y124$. Both compounds have the same number of 21 odd symmetry (infrared-active) phonon modes.

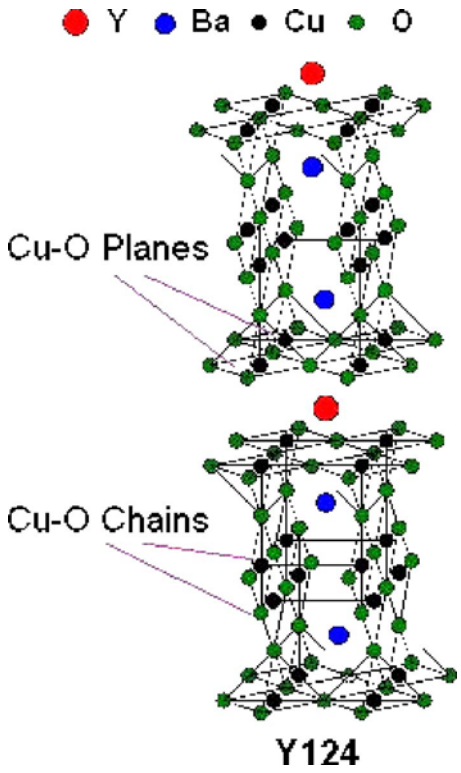

FIG. 1. (Color online) Crystallographic unit cell of $YBa_2Cu_4O_8$.

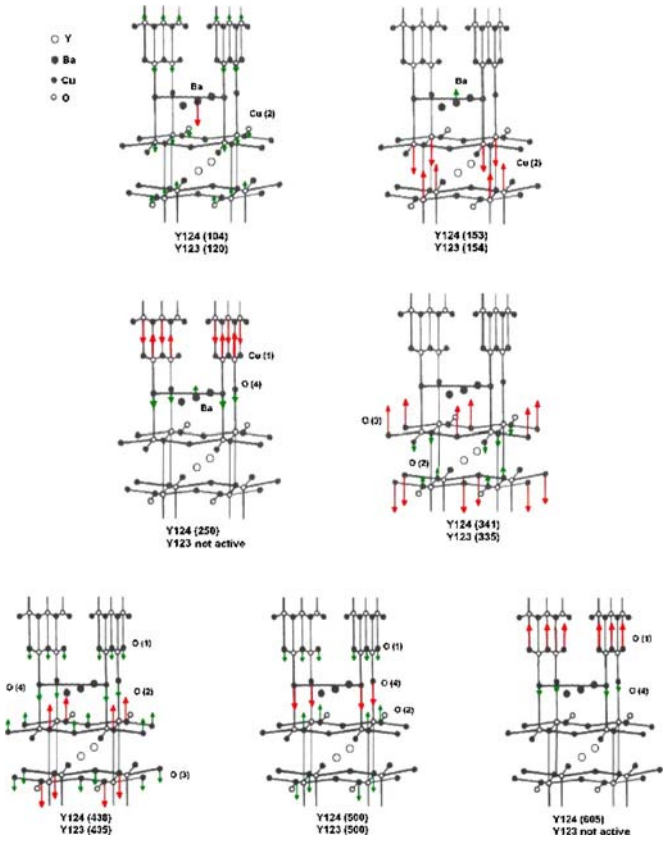

FIG. 2. (Color online) Displacement pattern of the calculated A_g Raman eigenmodes of $YBa_2Cu_4O_8$. The calculated eigenfrequencies are given in parentheses for *Y*124 and the corresponding modes in *Y*123.

Because of the technological difficulties in preparing high quality *Y*124 samples, especially single crystals, only a few reports on optical studies exist for this material. To the best of our knowledge, there existed until now no optical data for isotopically substituted *Y*124. Obhi *et al.*[17] reported that infrared absorption studies on *Y*124 powder diluted in CsI pellets, where they concentrated on the anomalous temperature dependence of the phonon modes in the vicinity of the SC transition. They also summarized previous reflectivity results by other authors[18–20] and compared the obtained phonon parameters with the predictions of shell model calculations.[21] Raman experiments on *Y*124 have been performed on single crystalline samples[22,23] as well as on ceramic ones.[24] The experimental investigation of isotopically substituted *Y*124 samples has been limited to nuclear magnetic resonance (NMR) studies,[25–27] where the emphasis was on the isotope effect of the so-called pseudogap in the normal state.

II. SAMPLES

The set of $YBa_2Cu_4O_8$ ceramic specimens made of different isotopically pure Cu, Ba, and O precursors have been used in our experiments (The same samples were examined by NMR (Refs. 25 and 27). Phase pure $YBa_2Cu_4O_8$ polycrystalline samples [as established by x-ray diffraction] were synthesized by means of a standard solid-state reaction from Y_2O_3, CuO, and $BaCO_3$ at 945 °C and 60 bars oxygen pressure. The pellet-shaped samples had a diameter of 12 mm and a thickness of a few millimeters. Samples with isotopes of copper 63 and 65 were made from isotopically pure ^{65}Cu and ^{63}Cu metals. CuO powder from each isotope was ob-

TABLE I. Calculated frequencies and eigenvectors of the A_g Raman-active modes of *Y*124. Underlined entries identify the strongest component of each eigenvector (Refs. 28 and 30).

Calculated (cm^{-1})	Assignment	Ba	Cu(2)	Cu(l)	O(3)−O(2)	O(3)+O(2)	O (4)	O(1)
576	O(l)	−0.02	+0.01	−0.49	−0.08	−0.06	−0.27	+0.82
489	O(4)	+0.01	−0.06	−0.13	+0.01	+0.56	−0.77	−0.29
426	O(3)+O(2)	+0.05	+0.13	−0.08	+0.33	+0.77	−0.47	−0.22
393	O(3)−O(2)	+0.01	+0.01	−0.03	+0.94	+0.27	+0.16	+0.14
270	Cu(l)	−0.22	−0.15	+0.83	+0.03	−0.03	−0.31	+0.39
169	Cu(2)	+0.33	−0.93	−0.08	+0.04	−0.11	+0.01	−0.02
89	Ba	−0.92	−0.29	−0.21	+0.03	−0.07	+0.06	−0.13

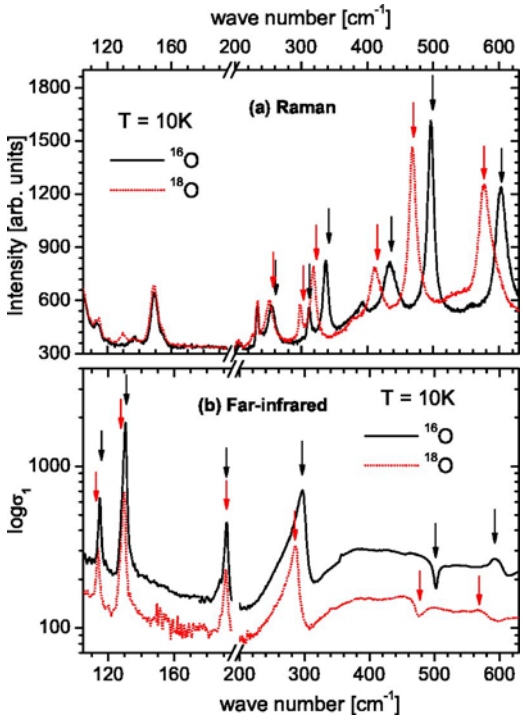

FIG. 3. (Color online) Raman scattering (a) and far-infrared ellipsometry (b) spectra for oxygen substituted $YBa_2Cu_4O_8$ measured at 10 K. The arrows indicate the isotope shifts of the corresponding phonon modes. (Please note the axis break and change of the scale.)

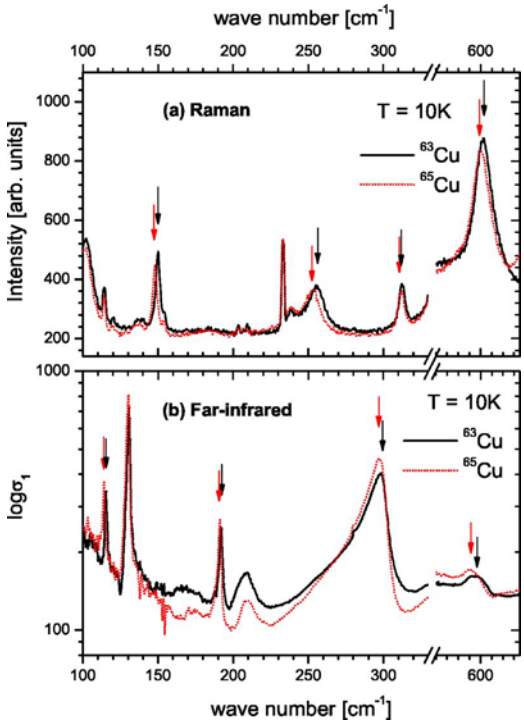

FIG. 4. (Color online) Raman scattering (a) and far-infrared ellipsometry (b) spectra for copper substituted $YBa_2Cu_4O_8$ measured at 10 K. The arrows indicate the isotope shifts of the corresponding phonon modes. (Please note the axis break.)

tained by dissolving the Cu metal in nitric acid followed by decomposing the nitrate at 700 °C in air. Barium samples were made of $BaCO_3$ powders with ^{130}Ba and ^{138}Ba isotopes. Unlike the ^{138}Ba sample, which contains almost 100% ^{138}Ba, the ^{130}Ba sample contains only 33% of this isotope (note that the natural abundance is only 0.1%), with the rest of the mass corresponding to other Ba isotopes, mainly ^{138}Ba (42%). To prepare samples with isotopically pure oxygen, a phase pure $YBa_2Cu_4O_8$ polycrystalline pellet was cut in two halves. One of them was annealed in ^{18}O while the other was treated under identical conditions in ^{16}O gas. Each sample was annealed in the same place of the furnace at 760 °C for 4*h*. The annealing was repeated with a fresh charge of ^{18}O. An estimate based on the mass change upon oxygen isotope replacement indicates that the ^{18}O sample contained 96% of ^{18}O.

III. EXPERIMENTAL METHODS

A. Raman scattering

Raman scattering measurements were made on a triple monochromator Jobin Yvon 64000 *X* spectrometer with a charge-coupled device detector in backscattering configuration. We used the 514.5 nm laser line of an Ar^+ laser as an excitation source. The samples were measured in pairs for each substituted element, thus ensuring identical experimental conditions during the measurement. The resolution of the spectrometer was set to 0.5 cm^{-1} (0.2 cm^{-1}) for the oxygen (Cu and Ba) substituted samples. All samples were examined at 10 and 100 K, additionally the oxygen isotope samples were studied at 300 K. The total laser power was about 30 mW with approximately 15 mW on the sample. The measurements were performed without polarizers; the recorded spectra should thus represent an average over all scattering configurations.

B. Far-infrared ellipsometry

The far-infrared ellipsometric measurements were performed with a homebuilt ellipsometer attached to a Bruker 113v Fourier-transform infrared spectrometer. Ellipsometry is a self-normalizing technique that yields directly the complex dielectric function without the need for a Kramers-Kronig analysis. The spectral range of the phonon modes from about 100 to 700 cm^{-1} was covered with three mylar beam splitters (3.5, 6, and 12 μm). A Hg-arc lamp served as a light source. The spectral resolution was set to 0.24 cm^{-1}. The measurements were performed at different temperatures of 10, 100, and 300 K. The ellipsometry data yield the complex reflectance ratio[16]

$$\tilde{\rho}(\omega,\phi) = \frac{\tilde{r}_p(\omega,\phi)}{\tilde{r}_s(\omega,\phi)}, \qquad (1)$$

where ϕ is the angle of incidence and $\tilde{r}_p$ and $\tilde{r}_s$ are the Fresnel reflection coefficients for *p*- and *s*-polarized light, respectively. In our experiment we used ϕ=80°. By transforming Eq. (1) we obtain the complex dielectric function[16]

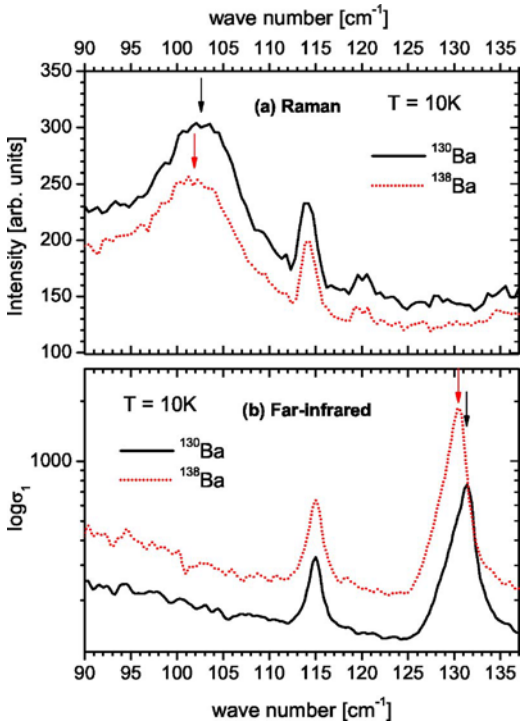

FIG. 5. (Color online) Raman scattering (a) and far-infrared ellipsometry (b) spectra for barium substituted $YBa_2Cu_4O_8$ measured at 10 K. The arrows indicate the isotope shifts of the corresponding phonon modes.

$$\tilde{\epsilon}(\omega) = \left(\frac{1-\tilde{\rho}(\omega,\phi)}{1+\tilde{\rho}(\omega,\phi)}\right)^2 \tan^2\phi \sin^2\phi + \sin^2\phi, \qquad (2)$$

where an isotropic, clean, and homogeneous sample surface is assumed. This assumption is reasonable since for ceramic grains all possible orientations contribute to the measured signal.

For $YBa_2Cu_4O_8$ crystals, which are highly anisotropic, the IR response for the c-axis is insulatorlike, with the phonon structures well visible, whereas the in-plane response is metalliclike, with the phonon features rather well screened. One, therefore, observes that, like for other HTSC polycrystalline pellets, the pseudodielectric function determined from the Eq. (2) is dominated by the phonon structures of the c-axis response.

IV. *AB INITIO* CALCULATIONS

One of the motivations for the present study was to test the predictions of the *ab initio* calculations obtained by the FP-LMTO (full potential linear muffin-tin-orbital) method based on the LDA (local density approximation).[28,29] Table I, extracted from Ref. 30, contains the theoretical eigenfrequencies (together with the experimental data for natural $Y124$) and eigenvectors of the A_g Raman-active modes of $Y124$.

The underlined entries indicate the strongest component of each eigenvector. The displacement patterns of the calculated A_g Raman eigenmodes for $YBa_2Cu_4O_8$ and the corresponding modes of $YBa_2Cu_3O_7$ are displayed in Fig. 2.

For the IR-active modes such *ab initio* calculations are presently not available. They are considerably more difficult than those of the Raman-active modes since the infrared modes have odd parity with respect to the inversion center.

V. RESULTS

A. Raman scattering

Figure 3(a) shows typical Raman spectra at 10 K for the $Y124$ samples with ^{16}O and the isotopically exchanged ones with ^{18}O.

The eigenfrequencies of the phonon modes in the Raman spectra were determined by fitting with Lorentzian profiles. The electronic background was modeled with polynomial

TABLE II. Position and full width at half maximum (FWHM) of the Raman-active phonon modes at 10 K for the oxygen isotope substituted samples. Also shown is the isotopic shift from experiment and theory, as well as the assignment of the phonon modes. [The frequency differences between isotopes were calculated using Eq. (3)]

^{16}O		^{18}O		Differences between ^{16}O–^{18}O		
Peak position [cm^{-1}]	Average FWHM [cm^{-1}]	Peak position [cm^{-1}]	Average FWHM [cm^{-1}]	Experiment [cm^{-1}]	Theory [cm^{-1}]	Assignment[a]
604.9	19.9	**580.3**	24.4	**24.6**	**26.3**	O(1)
498.3	10.9	**470.7**	13.0	**27.6**	**28.2**	O(4)
436.1	23.0	**413.6**	21.6	**22.5**	**24.3**	O(3)+O(2)
339.2	9.1	**320.2**	11.1	**19.0**	**19.4**	O(3)−O(2)
314.2	6.2	**300.8**	6.1	**13.3**	—	—
257.3	13.7	**253.8**	14.2	**3.5**	**3.8**	Cu(1)
151.3	5.6	151.4	6.1	−0.1	0.1	Cu(2)
104.5	10.1	104.6	9.6	−0.2	0.2	Ba

[a]Reference 30.

TABLE III. Position and full width at half maximum (FWHM) of the Raman-active phonon modes at 10 K for the copper isotope substituted samples. Also shown is the isotopic shift from experiment and theory, as well as the assignment of the phonon modes. [The frequency differences between isotopes were calculated using Eq. (3)]

^{63}Cu		^{65}Cu		Differences between ^{63}Cu–^{65}Cu		
Peak position [cm^{-1}]	Average FWHM [cm^{-1}]	Peak position [cm^{-1}]	Average FWHM [cm^{-1}]	Experiment [cm^{-1}]	Theory [cm^{-1}]	Assignment[a]
604.6	18.1	**602.3**	20.1	**2.3**	**2.3**	O(1)
498.5	9.8	498.3	10.7	0.2	0.2	O(4)
435.7	20.7	435.1	21.9	0.6	0.2	O(3)+O(2)
338.9	7.7	338.9	8.0	0	0	O(3)−O(2)
314.3	4.3	**313.5**	4.4	**0.8**	—	—
257.7	11.4	**254.8**	10.7	**2.9**	**2.9**	Cu(1)
151.7	3.0	**149.7**	3.5	**2.0**	**2.1**	Cu(2)
103.8	9.1	103.5	9.2	0.3	0.2	Ba

[a]Reference 30.

functions (to second order) and some plasma peaks from the laser source were described by Gaussian profiles. The mode energies of the natural sample agree reasonably well with the result of previous Raman experiments on $Y124$ single crystal[22] and polycrystalline[23] samples and are also comparable with the predictions of the semiempirical shell model calculations.[21] Only the 257 cm^{-1} mode exhibits a significant difference (about 5–7 cm^{-1}) from the previously reported values.

The Raman spectra exhibit four strong peaks at 605, 498, 436, and 339 cm^{-1} and four weaker ones at 314, 257, 151, and 104 cm^{-1}. Except for the peak at 357 cm^{-1}, which probably corresponds to a phonon with B_{3g} symmetry,[23] the remaining peaks are accounted for by A_g phonons. The sharp feature at 234 cm^{-1} corresponds to a laser plasma line which can be used to calibrate the energy axis. The arrows mark those phonon modes which exhibit a significant isotopic shift. The relative mass difference between the oxygen isotopes is rather large (as compared to the one of Cu and Ba). Correspondingly, the phonon modes with a substantial contribution of the oxygen ions should exhibit sizeable isotopic shifts. Evidently, this is realized for the six phonon modes at 605, 498, 436, 339, and 257 cm^{-1}. The corresponding Raman spectra for the Cu isotope substituted samples are displayed in Fig. 4(a). Here we can identify four phonon modes at 605, 314, 257, and 151 cm^{-1} which exhibit a copper isotope dependent shift. The comparison of the oxygen and copper related shifts suggests that the A_g phonon modes at 257 and 605 cm^{-1} as well as the B_{3g} phonon at 357 cm^{-1} correspond to oxygen-copper mixed modes. As shown in Fig. 5(a), for the barium isotopes we find a noticeable isotopic shift only for the A_g phonon mode at 104 cm^{-1}. Tables II–IV provide a list of the average experimental peak positions and widths of the resulting experimental isotopic shifts. They are

TABLE IV. Position and full width at half maximum (FWHM) of the Raman-active phonon modes at 10 K for the barium isotope substituted samples. Also shown is the isotopic shift from experiment and theory, as well as the assignment of the phonon modes. [The frequency differences between isotopes were calculated using Eq. (3)]

^{130}Ba		^{138}Ba		Differences between ^{130}Ba–^{138}Ba		
Peak position [cm^{-1}]	Average FWHM [cm^{-1}]	Peak position [cm^{-1}]	Average FWHM [cm^{-1}]	Experiment [cm^{-1}]	Theory [cm^{-1}]	Assignment[a]
604.5	19.6	604.7	22.6	−0.3	0.0	O(1)
498.4	10.3	498.5	11.6	−0.1	0.0	O(4)
436.4	21.3	437.1	21.5	−0.7	0.0	O(3)+O(2)
338.9	7.6	338.9	8.3	0.1	0.0	O(3)−O(2)
314.1	4.3	314.4	5.1	−0.2	—	—
256.9	10.6	257.1	11.6	−0.2	0.2	Cu(1)
151.2	2.8	151.2	3.4	0.0	0.2	Cu(2)
104.6	10.7	**103.4**	10.2	**1.2**	**1.0**	Ba

[a]Reference 30.

TABLE V. Peak position of the infrared-active phonon modes at 10 K and their differences for the oxygen isotope substituted $Y124$ samples. Also shown are the corresponding peak positions for ^{138}Ba $Y123$[16] and "natural" $Y124$[17] together with the mode assignment from shell-model calculations.[31,21]

$Y123$[a,b]		$Y124$[c,d]		^{16}O		^{18}O		
Peak position [cm^{-1}]	Assignment	Peak position [cm^{-1}]	Assignment	Peak position [cm^{-1}]	Error [cm^{-1}]	Peak position [cm^{-1}]	Error [cm^{-1}]	Differences between ^{16}O–^{18}O
560.27	Cu(1), O(4)	598	O(4), O(1)out of phase	**592.5**	0.3	**566.5**	0.3	**26**
	O(1), O(2), O(3)	512	O(1)	**502.4**	0.3	**476.6**	0.3	**25.8**
309.74	Cu(1), O(1)	364	O(2), O(3) in phase	**357**	0.3	**340.6**	0.3	**16.4**
274.73	O(2), O(3) out of phase	259	O(2), O(3)out of phase	**297**	0.3	**286.1**	0.3	**10.9**
194.1	Y, Cu(1), O(2), O(3) in phase	193	Y	191.56	0.07	191.34	0.17	0.22
154.41	Complex, Ba, Cu(1)	150	Complex, Ba	130.56	0.01	129.96	0.02	0.6
	Cu(2,3), Ba	121	Cu(2), Ba	**114.9**	0.02	**113.72**	0.02	**1.18**

[a]Reference 16.
[b]Reference 31.
[c]Reference 21.
[d]Reference 17.

then compared to the theoretical values based on the (FP-LMTO) method. The error in determining the peak position is estimated to be about 5–10 % of the full width at half maximum (FWHM). From the theoretically predicted eigenvectors, the isotopic shifts were calculated according to the formula[16]

$$\frac{\Delta\omega_n}{\bar{\omega}_n} = -\frac{\Delta m}{2\bar{m}}[|\xi_{i,x}|^2 + |\xi_{i,y}|^2 + |\xi_{i,z}|^2]. \quad (3)$$

Here $\bar{m}$ is an average mass of the pair of isotopes and Δm is the difference between their isotopic masses. Accordingly, $\bar{\omega}_n$ represents the frequency of mode n corresponding to the average mass while $\Delta\omega_n$ accounts for the one of the mass difference. Finally, $\xi_{i,j}$ gives the component of the orthonormal eigenvector of mode n for ith atom in the unit cell along the direction j, subject to the normalization:

$$\sum_i (|\xi_{i,x}|^2 + |\xi_{i,y}|^2 + |\xi_{i,z}|^2) = 1. \quad (4)$$

By using the theoretically predicted mode assignment we obtain a good agreement with the experimental values of the isotope shifts. Only the two Raman modes at 605 and 257 cm^{-1} exhibit a significant admixture of contributions from Cu and O. The other modes are either mostly due to O (498, 435, and 339 cm^{-1}), Cu (151 cm^{-1}), or Ba (104 cm^{-1}). Overall, the agreement between the theoretical predictions of the *ab initio* model and the experimental values is very good. Unfortunately, there are no theoretical calculations concerning the 357 cm^{-1} B_{3g} mode. Our experiments suggest that this mode is dominated by O, with some admixture of Cu.

B. Far-infrared ellipsometry

As was mentioned above, for polycrystalline samples far-infrared ellipsometry yields the real and imaginary parts of a pseudodielectric function which concerning the infrared-active phonons is dominated by the response of the c-axis polarized modes. This allows one to accurately determine the eigenfrequencies of the c-axis phonon modes and, in particular, their relative isotope shifts. On the other hand, one has to be rather cautious when interpreting the absolute values of the corresponding oscillator strength. The ellipsometric spectra in Figs. 3(b) and 5(b) are shown in terms of the optical conductivity (on a logarithmic scale to better visualize the phonon modes) which is related to the dielectric function according to the formula

$$\tilde{\sigma}(\omega) = -i\frac{\omega}{4\pi}[\tilde{\epsilon}(\omega) - 1], \quad (5)$$

where ω is the frequency of the incident light. From the experimental spectra of $\tilde{\epsilon}(\omega)$ we have obtained the phonon

TABLE VI. Peak position of the infrared-active phonon modes at 10 K and their differences for the copper isotope substituted $Y124$ samples. Also shown are the corresponding peak positions for ^{138}Ba $Y123$[16] and "natural" $Y124$[17] together with the mode assignment from shell-model calculations.[31,21]

$Y123$[a,b]		$Y124$[c,d]		^{63}Cu		^{65}Cu		
Peak position [cm^{-1}]	Assignment	Peak position [cm^{-1}]	Assignment	Peak position [cm^{-1}]	Error [cm^{-1}]	Peak position [cm^{-1}]	Error [cm^{-1}]	Differences between ^{63}Cu–^{65}Cu
560.27	Cu(1), O(4)	598	O(4), O(1)out of phase	**595.4**	0.3	**590.4**	0.3	**5**
	O(1), O(2), O(3)	512	O(1)	502.8	0.3	502.1	0.3	0.7
309.74	Cu(1), O(1)	364	O(2), O(3) in phase	356.3	0.3	356.3	0.3	0
274.73	O(2), O(3) out of phase	259	O(2), O(3) out of phase	**298.4**	0.3	**297.5**	0.3	**0.9**
194.1	Y, Cu(1), O(2), O(3)in phase	193	Y	**192.21**	0.08	**191.32**	0.1	**0.89**
154.41	Complex, Ba, Cu(1)	150	Complex, Ba	**131.02**	0.03	**130.49**	0.02	**0.53**
	Cu(2,3), Ba	121	Cu(2), Ba	**115.14**	0.03	**114.04**	0.03	**1.1**

[a]Reference 16.
[b]Reference 31.
[c]Reference 21.
[d]Reference 17.

parameters by fitting simultaneously the real and the imaginary parts of the $\tilde{\epsilon}(\omega)$ function with Lorentzian oscillators. With regard to the complicated background (probably coming from the contributions of in-plane components of the dielectric function) only low wave number phonons (115, 130, and 191 cm^{-1}) were fitted with Lorentzian curves with some simple background, whereas the peak positions of the rest were read out from the spectra.

The nonsymmetric or "Fano-like" shape of the phonon structures on σ_1 spectra for wave numbers higher than 200 cm^{-1} is typically observed even for single crystaline samples, e.g., in Ref. 32. The possible explanation could be either a Fano type interference of the phonon with a continuum of electronic excitations or the effect of local fields discussed, e.g., by Munzar *et al.*[6,33]

The ellipsometry spectra of the $Y124$ samples at the lowest temperature of 10 K (at higher temperature some of the modes are significantly broadened) are presented in the same sequence as the Raman spectra: Fig. 3(b) shows the spectra for O isotope samples, Fig. 4(b) those of the Cu isotopes, and Fig. 5(b) those of the Ba isotopes. In Fig. 3(b) one can identify seven B_{1u} type phonon modes which are located at 592, 502, 357, 297, 191, 130, and 115 cm^{-1}.

Interestingly, all of them, with the exception of the 191 cm^{-1} mode, exhibit a noticeable oxygen isotope dependent frequency shift thus indicating significant O contributions. It is rather surprising that the modes at 115 and 130 cm^{-1} contain a significant contribution of oxygen despite of their very low eigenfrequency. For the Cu isotope samples in Fig. 4(b) there is also a large number of phonon modes exhibiting an isotopic shift, i.e., the phonon modes at 592, 502, 357, 191, 130, and 115 cm^{-1} (except for the mode at 297 cm^{-1}). For the barium substituted samples of Fig. 5(b) only the 130 cm^{-1} mode is sensitive to the isotopic substitution. A general feature is that the infrared-active B_{1u} modes are more strongly mixed than the corresponding Raman modes. This can be easily understood in terms of the center of mass conservation, which for odd symmetry phonon modes requires the counter motion of a second kind of ions. The experimental results are summarized in Tables V–VII together with the theoretical predictions for "natural" $Y123$ and $Y124$ as obtained from the shell model calculations.

Most interesting is the comparison with the assignment of the phonon modes in $Y123$ as presented by Henn *et al.*[16] based on similar measurements for a complete set of isotopically substituted samples. These authors compared them with eigenvectors for the phonon modes in $Y123$, from the shell model calculations. According to their assignment, the three phonon modes at 310, 194, and 154 cm^{-1} involve mostly the displacement of the ions within the CuO_2-Y-CuO_2 bilayer block, which is equally present for the $Y124$ structure. We find that the phonon modes at 357, 191, and 130 cm^{-1} exhibit very similar isotopic shifts as the ones at 310, 190, and 150 cm^{-1} in $Y123$, in good agreement with the assignment of Henn *et al.*[16] This finding lends support to the conclusions of Henn *et al.*[16] and thus sets a firm basis for the

TABLE VII. Peak position of the infrared-active phonon modes at 10 K and their differences for the barium isotope substituted $Y124$ samples. Also shown are the corresponding peak positions for ^{138}Ba $Y123$[16] and "natural" $Y124$[17] together with the mode assignment from shell-model calculations.[31,21]

$Y123$[a,b]		$Y124$[c,d]		^{130}Ba		^{138}Ba		
Peak position [cm^{-1}]	Assignment	Peak position [cm^{-1}]	Assignment	Peak position [cm^{-1}]	Error [cm^{-1}]	Peak position [cm^{-1}]	Error [cm^{-1}]	Differences between ^{130}Ba–^{138}Cu
560.27	Cu(1), O(4)	598	O(4),O(1) out of phase	592.5	0.3	592.5	0.3	0
	O(1), O(2), O(3)	512	O(1)	502.4	0.3	502.4	0.3	0
309.74	Cu(1), O(1)	364	O(2), O(3) in phase	356.3	0.3	357	0.3	–0.7
274.73	O(2), O(3) out of phase	259	O(2), O(3) out of phase	297.2	0.3	297	0.3	0.2
194.1	Y, Cu(1), O(2), O(3) in phase	193	Y	191.64	0.1	191.56	0.07	0.08
154.41	Complex, Ba, Cu(1)	150	Complex, Ba	**131.6**	0.01	**130.56**	0.01	**1.04**
	Cu(2,3), Ba	121	Cu(2), Ba	114.82	0.02	114.9	0.02	–0.08

[a]Reference 16.
[b]Reference 31.
[c]Reference 21.
[d]Reference 17.

assignment of the infrared-active modes in $Y124$. For $Y123$ the remaining two modes at 280 and 565 cm^{-1} involve the displacement of ions within the CuO chain layer. As expected in $Y124$ the number of these modes is doubled (the four modes at 592, 502, 297, and 115 cm^{-1}), as required by the doubled number of CuO chain layers in $Y124$. The so-called apical mode at 565 in $Y123$ thus finds its correspondence in the highest modes at 592 and 502 cm^{-1} for $Y124$. For the so-called chain mode at 280 cm^{-1} in $Y123$ the respective modes are located at 297 and 115 cm^{-1} in $Y124$. The modes with lower frequency than in $Y123$ correspond here to the out-of phase vibration of the ions in the double CuO chains.

The self-consistence of the experimentally observed isotopic shifts has been checked via the summation of the element specific isotopic shifts as is shown in Table VIII. On theoretical grounds this sum should be equal to unity. Evidently, our experimental data fulfill this requirement within an accuracy of about 10%. The only exception concerns the phonon modes at 191 cm^{-1}, where this sum is much smaller than unity and at 592 cm^{-1}, where the sum is a bit larger then unity. For the first mode it is indeed well known that the Y ion provides an important contribution, which has not been accessed in our present experiments and the subsequent calculation. In return, the consistency for the other modes suggests that the Y ions do not provide a significant contribution. For the second mode the value is affected by large error bars, which comes from the broadness of that mode and the concomitant difficulties in pinpointing the position of its maximum.

VI. CONCLUSIONS

We have investigated by Raman and infrared spectroscopy the effects of Ba, Cu, and O substitution on the Brillouin center phonons of $YBa_2Cu_4O_8$ polycrystalline samples. The observed isotope shifts provide insight into their relative Ba, Cu, and O normal vibrational content. This allows us to examine mode eigenvectors obtained from lattice dynamical calculations based on *ab initio* electronic structures performed with the FP-LMTO within the LDA.

Our Raman results demonstrate that the 104 cm^{-1} A_g phonon is only very weakly mixed, representing almost pure Ba vibrations. Correspondingly, the 151 cm^{-1} phonon represents pure Cu vibrations. The 339, 436, and 498 cm^{-1} phonon modes correspond mainly to O vibrations. Considerable Cu-O mixing takes place in the case of the A_g phonons at 257 and 605 cm^{-1} and for the B_{3g} phonon at 314 cm^{-1}. These results are in good agreement with the *ab initio* calculations.

The infrared-active modes are, as expected, more strongly mixed. The modes with energies of 115, 297, 502, and

TABLE VIII. Normalized amplitudes for the ionic displacements of oxygen, copper, and barium as deduced from the far-infrared measurements on the isotope substituted $Y124$ samples according to Eq. (3).

Mode	$\lvert\xi_{Ba}\rvert$	$\lvert\xi_{Cu}\rvert$	$\lvert\xi_{O}\rvert$	$\lvert\xi_{Ba}\rvert^2+\lvert\xi_{Cu}\rvert^2+\lvert\xi_{O}\rvert^2$	Assignment[a]
592.5	0.00	0.73	0.89	1.33	O(4), O(1) out of phase
502.4	0.00	0.30	0.96	1.02	O(1)
357	0.41	0.00	0.91	1.00	O(2), O(3) in phase
297	0.24	0.44	0.81	0.91	O(2), O(3) out of phase
191.56	0.19	0.55	0.14	0.35	Y
130.56	0.82	0.51	0.29	1.01	Complex, Ba
114.9	0.24	0.78	0.43	0.86	Cu(2), Ba

[a]Reference 17.

592 cm^{-1} are mixed vibrations of O and Cu atoms. The phonon mode at 130 cm^{-1} corresponds to a Ba-Cu-O complex whereas the modes at 191 and 357 cm^{-1} reflect almost pure Cu and O vibrations, respectively. The comparison with the similar work of Henn *et al.*[16] on *Y*123 allows us to identify the modes at 130, 191, and 357 as involving mostly the CuO_2-Y-CuO_2 bilayer unit whereas the modes at 592, 502, 297, and 115 also involve the CuO double chain layer.

ACKNOWLEDGMENTS

One of us (A.T.) gratefully acknowledges the hospitality of the Max-Planck Institut für Festkörperforschung. The financial support of the Deutsche Forschungsgemeinschaft (DFG), Grant No. BE2684/1-2 in FOR 538 and the Schweizer Nationalfonds (SNF) through Project No. 200021-111690 are gratefully acknowledged.

[1] Z. B. Huang, W. Hanke, E. Arrigoni, and D. J. Scalapino, Phys. Rev. B **68**, 220507(R) (2003).

[2] O. Rösch and O. Gunnarsson, Phys. Rev. Lett. **92**, 146403 (2004); **93**, 237001 (2004).

[3] C. Castellani, C. DiCastro, and M. Grilli, Phys. Rev. Lett. **75**, 4650 (1995); F. Becca, M. Tarquini, M. Grilli, and C. Di Castro, Phys. Rev. B **54**, 12443 (1996).

[4] J. L. Tallon, R. S. Islam, J. Storey, G. V. M. Williams, and J. R. Cooper, Phys. Rev. Lett. **94**, 237002 (2005).

[5] C. Bernhard, T. Holden, A. V. Boris, N. N. Kovaleva, A. V. Pimenov, J. Humliček, C. Ulrich, C. T. Lin, and J. L. Tallon, Phys. Rev. B **69**, 052502 (2004).

[6] D. Munzar, C. Bernhard, A. Golnik, J. Humliček, and M. Cardona, Solid State Commun. **112**, 365 (1999).

[7] A. V. Boris, D. Munzar, N. N. Kovaleva, B. Liang, C. T. Lin, A. Dubroka, A. V. Pimenov, T. Holden, B. Keimer, Y. L. Mathis, and C. Bernhard, Phys. Rev. Lett. **89**, 277001 (2002).

[8] A. P. Litvinchuk, C. Thomsen, and M. Cardona, in *Physical Properties of High Temperature Superconductors IV*, edited by D. M. Ginsberg (World Scientific, Singapore, 1994), p. 375.

[9] M. Cardona, R. Liu, C. Thomsen, W. Kress, E. Schönherr, M. Bauer, L. Genzel, and W. König, Solid State Commun. **67**, 789 (1988).

[10] M. K. Crawford, W. E. Farneth, E. M. McCarron III, and R. K. Bordia, Phys. Rev. B **38**, 11382 (1988).

[11] C. Thomsen, A. P. Litvinchuk, E. Schönherr, and M. Cardona, Phys. Rev. B **45**, 8154 (1992).

[12] Zech, H. Keller, K. Conder, E. Kaldis, E. Liarokapis, N. Poulakis, and K. A. Müller, Nature (London) **371**, 681 (1994).

[13] A. Mascarenhas, H. Katayama-Yoshida, J. Pankove, and S. K. Deb, Phys. Rev. B **39**, 4699 (1989).

[14] J. C. Irwin, J. Chrzanowski, E. Altendorf, J. P. Franck, and J. Jung, J. Mater. Res. **5**, 2780 (1990).

[15] T. Strach, T. Ruf, E. Schönherr, and M. Cardona, Phys. Rev. B **51**, 16 460 (1995).

[16] R. Henn, T. Strach, E. Schönherr, and M. Cardona, Phys. Rev. B **55**, 3285 (1997).

[17] H. S. Obhi, E. K. Salje, and T. Miyatake, J. Phys.: Condens. Matter **4**, 10367 (1992).

[18] R. G. Buckley, M. P. Staines, and H. J. Trodahl, Physica C **185-189**, 977 (1991).

[19] M. E. Ziaei, B. P. Clayman, R. G. Buckley, and M. P. Staines, Physica C **176**, 242 (1991).

[20] P. Litvinchuk, C. Thomsen, P. Murugaraj, and M. Cardona, Z. Phys. B: Condens. Matter **86**, 329 (1992).

[21] K. K. Yim, J. Otimaa, and M. M. Elcombe, Solid State Commun. **77**, 385 (1991).

[22] M. C. Krantz, H. J. Rosen, R. M. MacFarlane, N. G. Asmar, and D. E. Morris, Physica C **162-164**, 1089 (1989).

[23] E. T. Heyen, R. Liu, C. Thomsen, R. Kremer, M. Cardona, J. Karpinski, E. Kaldis, and S. Rusiecki, Phys. Rev. B **41**, 11058 (1990).

[24] P. Litvinchuk, C. Thomsen, and M. Cardona, Solid State Commun. **83**(5), 343 (1992).

[25] G. V. M. Williams, J. L. Tallon, J. W. Quilty, H. J. Trodahl, and N. E. Flower, Phys. Rev. Lett. **80**, 377 (1998).

[26] F. Raffa, T. Ohno, M. Mali, J. Roos, D. Brinkmann, K. Conder, and M. Eremin, Phys. Rev. Lett. **81**, 5912 (1998).

[27] G. V. M. Williams, D. J. Pringle, and J. L. Tallon, Phys. Rev. B **61**, R9257 (2000).

[28] F. Paulsen (unpublished).

[29] B. Lederle, Ph.D. thesis, Max Planck Institute, Stuttgart, 1997.

[30] M. Cardona, in *Raman Scattering In Materials Science*, edited by W. H. Weber and R. Merlin (Springer-Verlag, Berlin, 2000), Chap. 5.

[31] J. Humliček, A. P. Litvinchuk, W. Kress, B. Lederle, C. Thomsen, M. Cardona, H. U. Habermeier, I. E. Trofimov, and W. König, Physica C **206**, 345 (1993).

[32] D. N. Basov, T. Timusk, B. Dabrowski, and J. D. Jorgensen, Phys. Rev. B **50**, R3511 (1994).

[33] D. Munzar, J. Phys. Chem. Solids **67**, 308 (2006).